03

Interferometry of optical vortices in the presence of spatial phase noise

© D.D. Reshetnikov, T.K. Korol, E.V. Malyutina, V.M. Petrov

St. Petersburg State University,
St. Petersburg, Russia

e-mail: d.d.reshetnikov@gmail.com

Received June 13, 2024
Revised July 20, 2024
Accepted July 29, 2024

A method for recording interferograms of optical beams with orbital angular momentum (OAM) is proposed. Interferograms are formed due to interference of the zero and one of the first orders of beam diffraction when an additional diffraction grating is added into the optical scheme. The noise robustness of such a detection method has been experimentally and theoretically investigated using the addition of OAM beams with two-dimensional phase noise. The Gaussian distribution was used to describe the phase noise. The magnitude of its standard deviation σ varied during measurements. For these specific conditions of our experiment, the limiting value σ was determined, which makes it possible to register the value of the OAM according to the criterion $S/N = 3$.

Keywords: optical vortices, beams with phase noise, registration of optical vortices, light with orbital angular momentum, spatial light modulator.

DOI: 10.61011/EOS.2024.07.59649.6774-24

Introduction

Beams with axially-symmetric polarization structure or so-called optical vortices are of interest due to the extensive development of optical, in particular, quantum free-space, i.e. atmospheric, communication links [1–3]. Although such links provide communication only within line-of-sight range, they are of great interest for a variety of applications, for example, satellite communications between mobile objects, etc. [4,5]. This is associated with one of the key advantages of beams with axially-symmetric structure, i.e. invariance to unpredictable rotation of their polarization plane with respect to the propagation axis [6,7].

At this point, a significant number of theoretical and experimental studies has been performed in this area, including establishment of a quantum communication line protocol using axially-symmetric beams that is similar to BB84 used for linear polarization beams [8,9].

This study will focus on the influence of spatial phase noise on optical vortex detectability by a two-dimensional photodetector. Quite similar objectives occur, for example, in propagation of optical vortices through various turbulent media [10–15].

Another objective includes practical detection of OAM beams. There are several OAM beam detection techniques. They include: q-plates, crossed cylindrical lenses, two-dimensional phase light modulators (SLM) or holographic diffraction elements [16], including those based on various controlled (i.e. dynamic) holographic gratings [17–19]. OAM sorter technology is being rapidly developed now and is used to distinguish such beams in a wide range of values [20,21]. Extensive efforts are taken to use graphene and graphene-like coatings as photodetectors for the above-mentioned objectives [22,23].

Various approaches differ in beam detection rate, optical system dimensions and cost which drives into selecting an individual detection method for each particular application.

This paper proposes a technique of interferometric detection of optical vortices and illustrates the efficiency of this technique by signal-to-noise ratio measurement in the presence of spatial, i.e. two-dimensional, phase noise.

Experiment

A so-called „fork“ image that occurs as a result of background wave and vortex interference is one of the attributes of optical vortex. For this, interference between the zero and one of the first diffraction orders obtained due to additional introduction of a diffraction grating into the initial phase distribution of the Laguerre-Gaussian beam [24].

The test setup is shown in Figure 1. A spatial, i.e. two-dimensional light modulator (*4*) (SLM — Spatial Light Modulator) based on a LCoS (Liqud Crystal on Silicon) matrix is the main component. The matric had 1920×1080 pixels $8.0 \times 8.0\,\mu\mathrm{m}^2$ in size, the matrix aperture size is $15.36 \times 8.64\,\mathrm{mm}^2$ and the reflection coefficient is $65-95\%$. The modulator was connected via the HDMI port to PC (*8*) as a secondary additional monitor. Optical phase in each pixel was encoded using 256 levels (8 bit).

Additive mixture of three phase distributions was formed on the modulator aperture:

$$IN(x, y) = LG_{11}(x, y) + N(x, y) + G(x),$$

where x and y are the modulator matrix coordinates (Figure 2). Method of constructing a similar mask is described in [25].

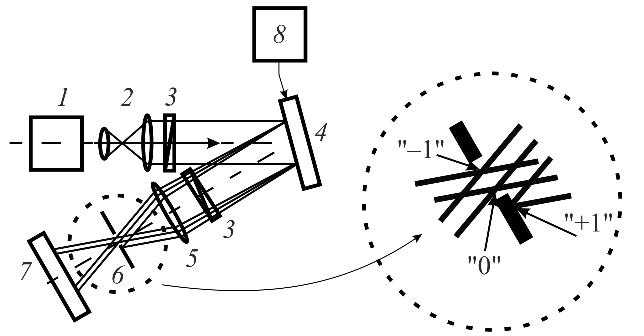

Figure 1. Experimental setup. *1* — laser, $\lambda = 650\,\text{nm}$, $2\,\text{mW}$; *2* — beam expander; *3* — polarizer and analyzer; *4* — two-dimensional light modulator; *5* — lens, $F = 300\,\text{mm}$; *6* — spatial filter; *7* — CCD camera; *8* — PC. The inset shows the position of the spatial filter transmitting the zero and one of the first diffraction orders.

Distribution $LG_{p,l}(x, y)$ consists of $p + 1$ concentric rings with zero field intensity in the center of beam at $l \neq 0$ that is referred to as the point of singularity. Fields between neighboring rings are also equal to zero.

Distribution $N(x, y)$ defined the two-dimensional image of two-dimensional phase noise (Figure 3). It was built as follows: first, the screen was divided into 5×5 pixel squares. Then each square was encoded with a gray level using a value from 0 to 255 on the RGB scale. Gray level encoding values of each square were generated randomly using the Gaussian distribution with a mean value of 128 and mean-square deviation σ. By varying σ, the signal-to-noise ratio could be varied to simulate various values of spatial phase noise.

Distribution $G(x)$ represented a one-dimensional phase diffraction grating with the period $T(x)$ consisting of 10 pixels ($80\,\mu$m). The presence of such diffraction grating provided a pair of symmetric diffraction orders in the focal plane of the lens (*5*). The output image $OUT(\nu, \xi)$ was recorded using the CCD camera (*7*). The spatial filter (*6*) transmitted the zero and one of the first diffraction orders. The CCD camera (*7*) recorded the interference result. Recording plane (CCD camera plane) coordinates are designated as ξ and ν, respectively (Figure 4, *a*). The structure of the so-called „fork" in the interferogram indicates the optical vortex order. Two teeth in it indicate that the recorded wave is the first-order optical vortex ($l = 1$), three teeth — indicate the second-order vortex ($l = 2$), etc.

Figure 4, *b* shows the interferogram cross-section along the line $A{-}A$ in a relatively small output coordinate variation range $\Delta\xi$, i.e. in the nearest proximity of the „fork".

To describe quantitatively the efficiency of detection of the additive optical vortex and two-dimensional phase noise mixture, we used the following method or estimating the signal-to-noise ratio S/N (Figure 5, *a*). First, the outer and inner boundaries of two first rings were determined. For the purpose of illustration, in Figure 5, *a* the outer boundary of the second ring is designated as $\Delta\xi$, within which S/N was estimated. These boundaries were not varied in all following experiments. To determine the value of S, the average over the amplitudes of all interference bands included in the rings was calculated:

$$S = \frac{1}{n}\sum_{i=1}^{n} S_i,$$

where S_i is the amplitude of the i-th interference band included in rings, n is the total number of interference bands within the rings in the scan image.

To determine the value of N, the average over the amplitudes of interference bands included in the areas between the rings was calculated:

$$N = \frac{1}{m}\sum_{i=1}^{m} N_i,$$

where N_i is the amplitude of the i-th interference band included in the areas between the rings, m is the total number of interference bands between the rings in the scan image.

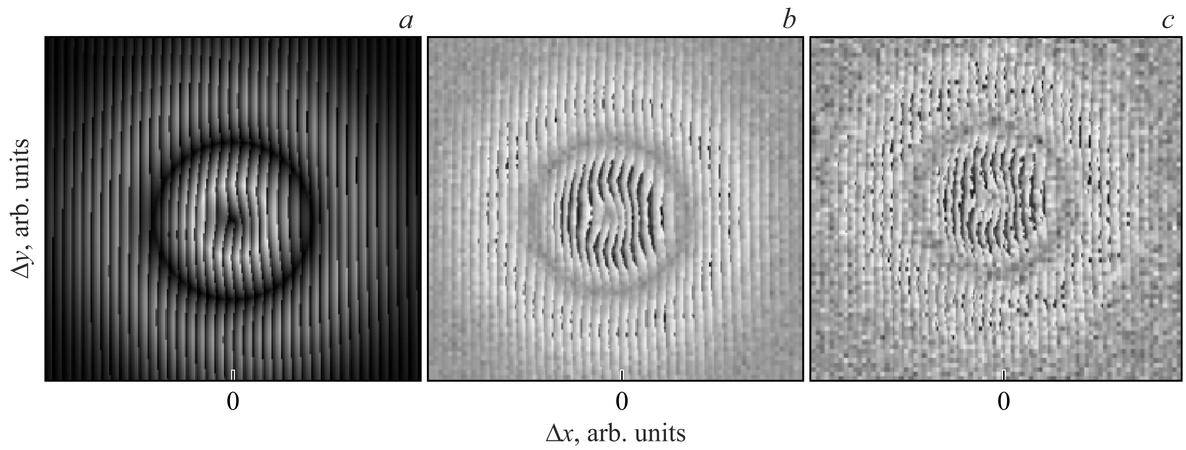

Figure 2. Examples of input phase distributions $IN(x, y)$ formed on the modulator screen. a — $\sigma = 0$, b — $\sigma = 10$, c — $\sigma = 20$.

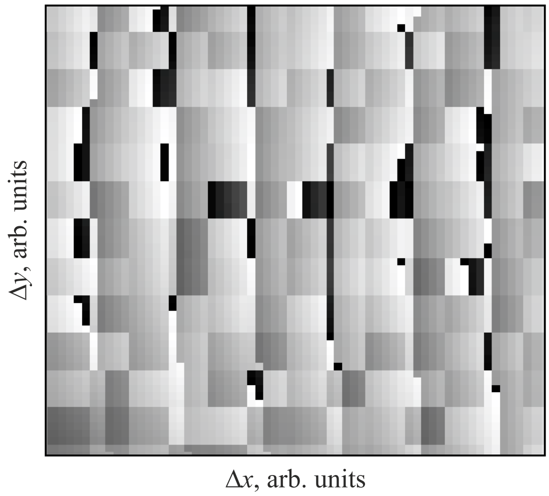

Figure 3. Part of input phase noise image $IN(x, y)$ for $\sigma = 20$.

Note that, in the ideal case, interference in the areas between the rings shall not be observed because the field between the rings is equal to zero. However, interference bands between the rings specifically indicates the presence of noise of different origin.

The above-mentioned algorithm was used to measure S/N for $\sigma = 0, 1, 2, 3, 4, 5, 10, 15, 20$. Figure 5, *a–e* shows the interference patterns and their scan images for $\sigma = 0, 1, 3, 10, 20$.

Simulation

Simulation of beam propagation with two-dimensional phase noise was performed using the second-order split-step beam propagation method SSBPM [26]. This method, in particular, allows the beam diffraction and irregularity effects induced by the two-dimensional phase noise to be addressed simultaneously. Flow chart of the algorithm is shown in Figure 6.

Masks displayed on SLM in the real experiment were used as phase screens. Beam propagation on a distance of 1 km with one phase screen in the middle of the optical path was simulated. Note that more phase screens are generally used to simulate the optical beam propagation through a turbulent medium by the SSBPM method, however, in our case, to meet the experiment conditions, only one phase screen was used to simulate OAM beam propagation in free space in the presence of phase noise. Beam diameter in the waist was equal to 2.4 mm, wavelength was equal to 650 nm. The beam transmitted through the optical path with the phase screen interferes in the Mach-Zehnder scheme with the reference Gaussian beam at an angle of 2.1 mrad to achieve an interference pattern containing the „fork“. The simulation provided scanned interference patterns on which S/N were found in the same way as described above (Figure 7, curve *2*). The measurements of S/N are also shown in Figure 7 (curve *1*).

Note that simulation provides a better S/N for various reasons. On the one hand, resolution of the pixel grid used for simulation is higher that of the camera, thus, the optical beam detection noise may be reduced. Pixel grid resolution used for simulation is also higher than the SLM resolution, which enables a more clearly-defined spatial beam profile to be formed. Finally, the simulation does not consider natural distortions and loss induced by optical components, imperfection of the initial laser beam wave front and beam diffraction on the SLM edges.

Conclusion and discussion of findings

Interferometric recording used in this study makes it possible to determine the presence of optical vortex even in conditions of quite high spatial phase noise. Such experiment apparently doesn't allow full-scale simulation

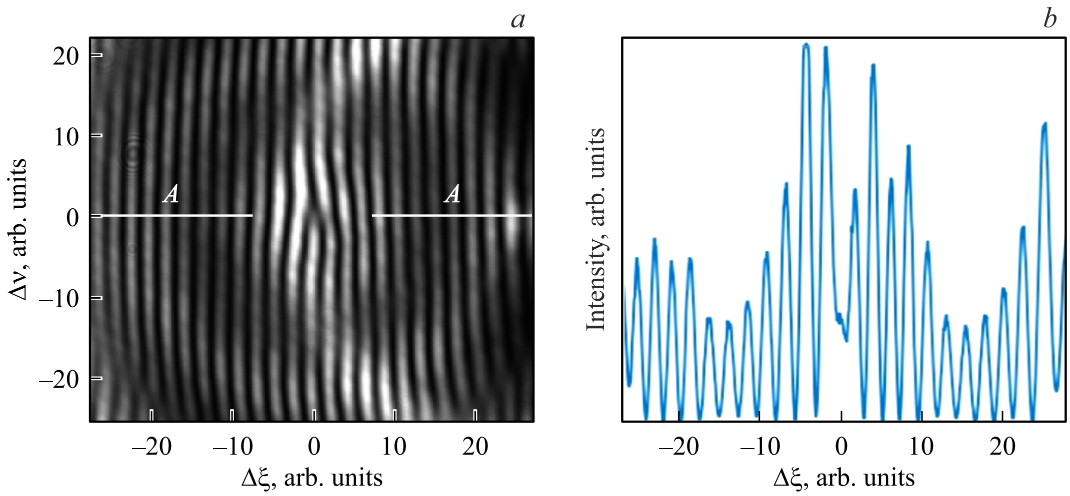

Figure 4. *a* — interferogram of the output Laguerre-Gauss beam $OUT(\nu, \xi)$, for $\sigma = 0$ within $\Delta\xi \pm 28$ *b* — cross-section on *A–A*.

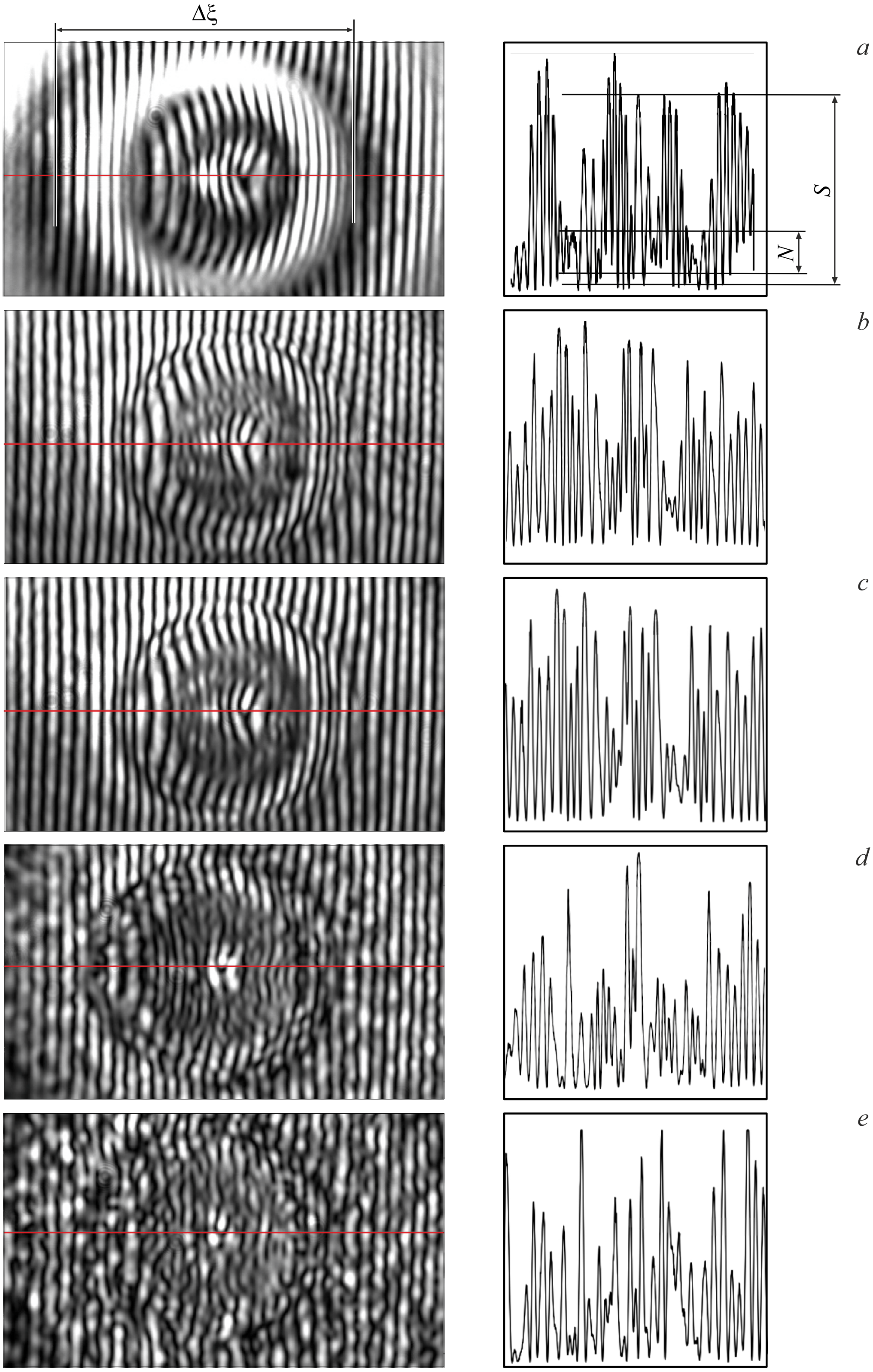

Figure 5. Left: interferograms of the output Laguerre-Gauss beam OUT(ν, ξ), right: interferogram cross-section in the outer boundary interval of the second beam cross-section ring $\Delta\xi$ consecutively for $\sigma = 0$ (a), 1 (b), 3 (c), 10 (d), 20 (e).

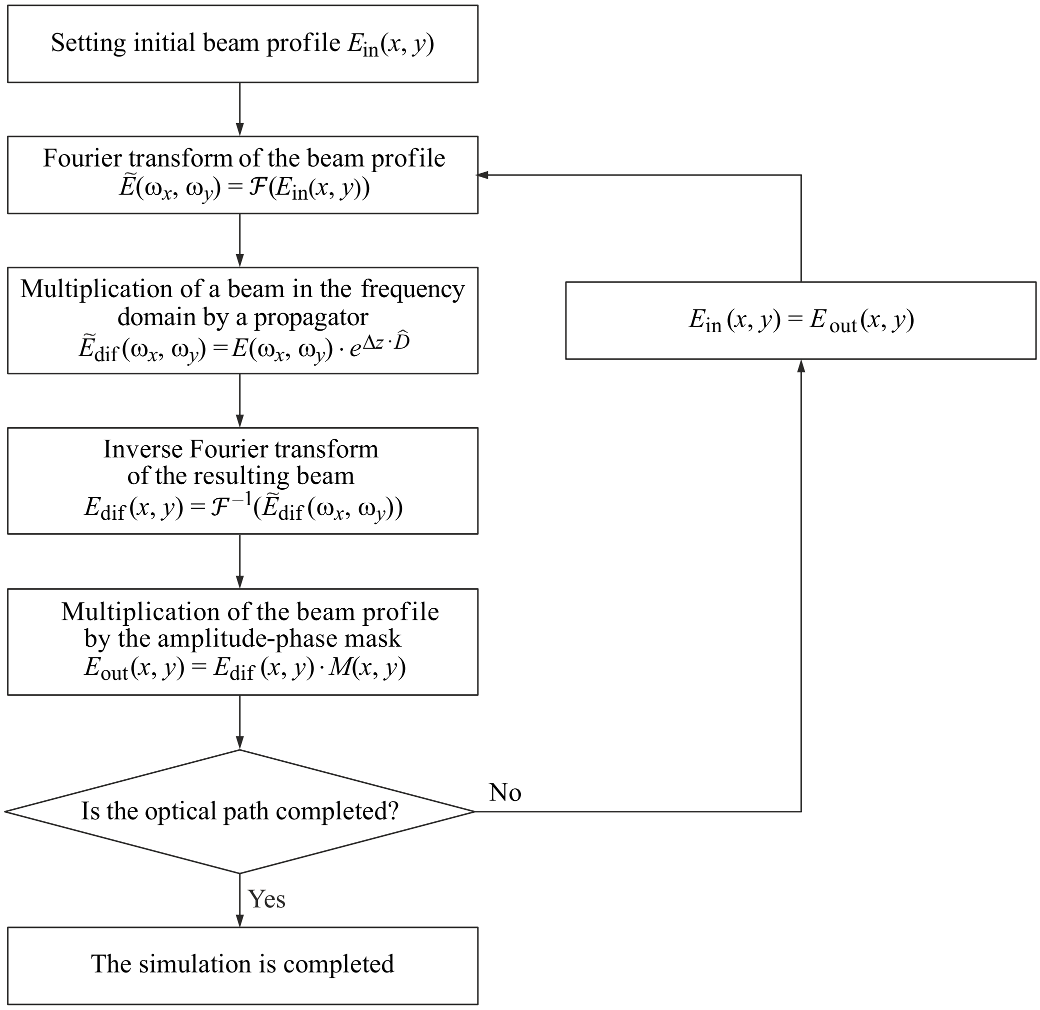

Figure 6. Flow chart of the simulation algorithm for optical beam propagation in a turbulent medium SSBPM.

of medium simulation because for this N two-dimensional phase modulators defining phase distributions in N discrete planes would have been arranged successively in axial alignment. However, the simulation results suggest that the proposed approach is easy to use for testing real optical systems.

As can be seen from the findings in Figure 7, the technique described above may be used to identify the fact of optical vortex detection by the criterion $S/N = 3$ at $\sigma = 10$. It is interesting to note that, even at higher σ: 10 and 20, the optical vortex interference pattern image can be identified (Figure 5, *d, e*), though in these cases $S/N < 3$, which doesn't meet the reliable detection criterion. Description of spatial phase noise using the Gaussian distribution is one of the most complicated cases compared with other models. Thus, the obtained estimate of σ is an upper-bound estimate.

The proposed interferometric detection method may be used in the development of data transmission systems in atmospheric optical links because the method of OAM beam data encoding allows the data capacity of such links to be increased cinsiderably. On the other hand, the shown

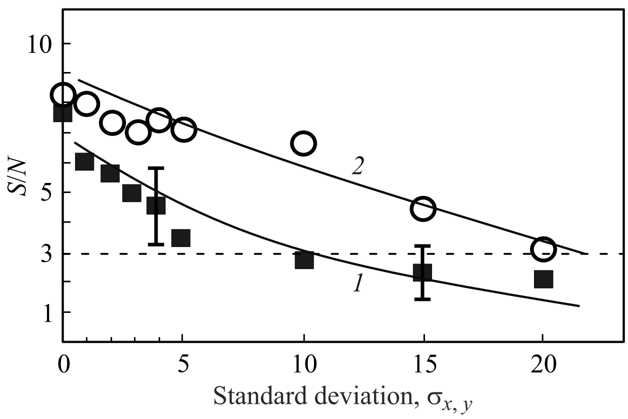

Figure 7. Dependence of S/N on the RMS deviation of phase noise in the Gaussian distribution: *1* — experiment, *2* — simulation.

simulation of beam propagation with OAM and spatial phase noise makes it possible to estimate the noise limit at which the atmospheric link may be effectively used for data transmission, including quantum key distribution problems where noise in a communication link is of essential to ensure the security of data to be transmitted.

Conflict of interest

The authors declare that they have no conflict of interest.

References

[1] J. Wang, J. Liu, S. Li, Y. Zhao, J. Du, L. Zhu. Nanophotonics, **11** (4), 645 (2022). DOI: 10.1515/nanoph-2021-0527

[2] J. Wang. Photon. Res., **4** (5), B14 (2016). DOI: 10.1364/PRJ.4.000B14

[3] A.E. Willner, K. Pang, H. Song, K.H. Zou, H.B. Zhou. Appl. Phys. Rev., **8** (4), 041312 (2021). DOI: 10.1063/5.0054885

[4] Z. Wang, R. Malaney, J. Green. IEEE Global Communications Conference (GLOBECOM), **1** (2019). DOI: 10.1109/GLOBECOM38437.2019.9014321

[5] L. Li, R. Zhang, Z. Zhao et al. Sci. Rep., **7**, 17427 (2017). DOI: 10.1038/s41598-017-17580-y

[6] A.L. Sokolov. J. Opt. Soc. Am. A., **30** (7), 1350 (2013). DOI: 10.1364/JOSAA.30.001350

[7] A.S. Akentiev, M.A. Sadovnikov, A.L. Sokolov, G.V. Simonov. Opt. i spektr., **122** (6), 1044 (2017) (in Russian). DOI: 10.7868/S0030403417060022

[8] A.L. Sokolov, V.M. Petrov, V.Yu. Venediktov, D.D. Reshetnikov. Fotonika, **17**, 7 (542) (2023). (in Russian). DOI: 10.22184/1993-7296.FRos.2023.17.7.542.555

[9] D.D. Reshetnikov, A.L. Sokolov, E.A. Vashukevich, V.M. Petrov, T.Yu. Golubeva. Izv. vuzov. Radiofizika, **67**(1), 58 (2024) (in Russian). DOI: 10.52452/00213462_2024_67_01_58

[10] V.P. Lukin. UFN, **191** (3), 292 (2021). [V.P. Lukin. Phys. Usp., **64** (3), 280 (2021). DOI: 10.3367/UFNr.2020.10.038849].

[11] A. Klug, C. Peters, A. Forbes. Adv. Photon., **5** (1), 016006 (2023). DOI: 10.1117/1.AP.5.1.016006

[12] S. Wabnitz. Opt. Lett., **39** (6), 1362 (2014). DOI: 10.1364/OL.39.001362

[13] M. Vorontsov, G. Carhart, R. Gudimetla et al. Proc. of the Advanced Maui Optical and Space Surveillance Technologies Conf., E18 (2010).

[14] R. Barros, S. Keary, L. Yatcheva, I. Toselli, S. Gladysz. Conference: Proc. SPIE 9242, Remote Sensing of Clouds and the Atmosphere XIX; and Optics in Atmospheric Propagation and Adaptive Systems XVII, **9242**, 92421L (2014). DOI: 10.1117/12.2070694

[15] L. Andrews, R. Phillips. *Laser Beam Propagation through Random Media, Second Edition* (SPIE Publications, Bellingham, Washington, 2005).

[16] D.M. Fatkhiev, M.A. Butt, E.P. Grakhova et al. Sensors, 21 (15), 4988 (2021). DOI: 10.3390/s21154988

[17] M.P. Petrov, V.M. Petrov, I.S. Zouboulis, L.P. Xu. Opt. Comm, **134** (1–6), 569 (1997). DOI: 10.1016/S0030-4018(96)00370-7

[18] V.M. Petrov, S. Lichtenberg, J. Petter, T. Tschudi. Opt. Comm., **229** (1–6), 131 (2004). DOI: 10.1016/j.optcom.2003.10.049

[19] S.M. Shandarov, S.S. Shmakov, N.I. Burimov, O.S. Syvaeva, Yu.F. Kargin, V.M. Petrov. JETP Letters, **95** (12), 618 (2012). DOI: 10.1134/S0021364012120144

[20] J. Cheng, C. Wan, Q. Zhan. Opt. Express, **30** (10), 16330 (2022). DOI: 10.1364/OE.455987

[21] H. Huang, G. Milione, M. Lavery et al. Sci Rep., **5**, 14931 (2015). DOI: 10.1038/srep14931

[22] G.L. Klimchitskaya, C.C. Korikov, V.M. Petrov. Phys. Rev. B, **92**, 159906(E) (2016). DOI: 10.1103/PhysRevB.93.159906

[23] G.L. Klimtchitskaya, V.M. Mostepanenko, V.M. Petrov. Phys. Rev. A, **98** (2), 023809 (2018). DOI: 10.1103/PhysRevA.98.023809

[24] J.A. Davis, D.M. Cottrell, J. Campos, M.J. Yzuel, I. Moreno. Appl. Opt., **38** (23), 5004 (1999). DOI: 10.1364/AO.38.005004

[25] E. Bolduc, N. Bent, E. Santamato et al. Optics Letters, **38** (18), 3546 (2013). DOI: 10.1364/OL.38.003546

[26] Y.K. Chahine, S.A. Tedder, B.E. Vyhnalek, A.C. Wroblewski. Free-Space Laser Communications XXXII. San Francisco, California, US, **11272**, 1127215 (2020). DOI: 10.1117/12.2543583

Translated by E.Ilinskaya